Reactions of small carbon anions with hydrogen sulfide, benzenethiol and sulfur

Keith Fisher,* Femia Hopwood, Ian Dance and Gary Willett

School of Chemistry, University of New South Wales, Sydney 2052, Australia.
E-mail: K.Fisher@unsw.edu.au

Received (in Montpellier, France) 19th January 1999, Accepted 24th March 1999

Carbon anions C_n^- ($n = 4$–13, 15–25 odd values only), generated by laser ablation of graphite or petroleum coke and isolated by Fourier transform ion cyclotron resonance mass spectrometry, have been reacted with the sulfur-containing molecules H_2S, C_6H_5SH and S_8. The C_n^- are unusually reactive with these molecules and generate anions of the types C_nS^-, $C_nS_2^-$, HC_nS^-, $C_nH_3S^-$, $C_nC_6H_5SH_2^-$, and $C_4S_3^-$. The structures of C_nS^-, $C_nS_2^-$ and HC_nS^- ($n = 4$–9) have been investigated by density functional calculations; the lowest energy isomers have linear structures with the hetero atom(s) at the end(s) of the chain. $C_4S_3^{-,0}$ are linear SC_4S–S species with a single S–S bond. The thioformyl molecule HCS, recently proposed to be involved in the collision of the comet Shoemaker–Levy with Jupiter, is believed to be a product in the reaction of C_9^- with H_2S.

A plethora of physical measurements on small carbon anions including anion photoelectron spectroscopy,[1] zero electron kinetic energy spectroscopy (ZEKE),[2] matrix isolation, electron detachment studies[3] and gas phase ion chromatography[4] suggest that C_2^- to C_9^- are linear. Theoretical calculations also indicate that the smaller carbon anions C_2^- to C_9^- are linear[5] and at high temperatures anions up to C_{13}^- may also be linear.[6] The linear anions C_{odd}^- have lower electron affinities than C_{even}^- and so it has been predicted that the linear C_n^- anions have cumulene structures when n is odd and polyacetylenic structures when n is even.[6] The anions with $n > 9$ are predicted to be cyclic although linear isomers may occur.[7] The reactivity of the anions should be related to structure, with linear anions being more reactive than cyclic anions. The carbon anions are observed to be relatively unreactive when compared to similar size cations and so initial reactivity studies were carried out with highly reactive molecules such as F_2 and C_2N_2[6] and O_2.[8] We have shown that the small carbon anions C_n^- ($n \leqslant 9$) are reactive towards 'less reactive' gaseous molecules such as H_2S[9] and P_4.[10] In the reactions of P_4 with C_n^- the reactivity reduced markedly at C_{10}^- and in reactions of C_n^- with H_2S[9] and P_4[10] the anions showed decreasing reactivity with increasing size and differing reaction products for even- and odd-numbered carbon anions.

We have now extended our investigations of the reactions of C_n^- to include S_8 and PhSH, and also larger carbon anions: these results are reported in this paper. We have also performed density functional calculations on many of the ions observed in the mass spectrometric experiments. The objective is to identify structural patterns in the heteroatom addition products of the carbon anions. Our previous calculations showed that the $[C_nP]^-$ and $[PC_nP]^-$ anions were linear,[10] similar to the $[C_nN]^-$ anions,[11] the silicon carbon anions[12] $[SiC_4]^-$, and $[SiC_5]^-$ and recently calculated neutral C_nS molecules.[13]

This work has some relevance to astronomical observations of carbon sulfide molecules in interstellar space,[14] and even more with the reactions occurring when the comet Shoemaker–Levy hit Jupiter.[15] We also note that there is a developing chemistry of carbon sulfide binary anions in the condensed phase:[16] species such as $C_2S_4^{2-}$, $C_3S_5^{2-}$ and $C_4S_6^{2-}$ are sulfur-rich relative to the species we observe in the gas phase.

Results

Reactions with H_2S

The reactions of H_2S with carbanions C_4^- to C_9^- have previously been reported.[9] The reactions of H_2S with carbanions C_n^- for $n = 10$–13 and 15–25 (odd values) have now been studied and the reactions for all the carbanions (including $n = 4$–9) are summarized by eqns (1)–(11), where eqns (7)–(10) represent reactions involving the formation of secondary ions. Table 1 illustrates the n-dependence of the product types for n up to 13.

$$C_n^- + H_2S \rightarrow \text{no ions} \qquad n = 10, 12 \tag{1}$$

$$C_n^- + H_2S \rightarrow \text{no reaction} \qquad n = 15, 17, 19, 21, 23, 25 \tag{2}$$

$$C_n^- + H_2S \rightarrow HS^- \qquad n = 4\text{–}9, 11, 13 \tag{3}$$

$$C_n^- + H_2S \rightarrow C_nH^- \qquad n = 4\text{–}9, 11, 13 \tag{4}$$

$$C_n^- + H_2S \rightarrow C_nHS^- \qquad n = 4\text{–}9 \tag{5}$$

$$C_n^- + H_2S \rightarrow C_nH_2S^- \qquad n = 9, 11, 13 \tag{6}$$

$$C_n^- + H_2S \rightarrow C_nH_3S^- \qquad n = 8, 9 \tag{7}$$

$$C_n^- + H_2S \rightarrow C_nH_3S_2^- \qquad n = 9 \tag{8}$$

$$C_n^- + H_2S \rightarrow C_{n-1}H_3S^- \qquad n = 9, 11, 13 \tag{9}$$

$$C_n^- + H_2S \rightarrow C_{n-4}S_2^- \qquad n = 7, 9 \tag{10}$$

$$C_n^- + H_2S \rightarrow C_{n-1}H^- \qquad n = 7, 9 \tag{11}$$

We now outline the significant features of these reactions.

(*a*) C_{10}^- and C_{12}^- anions reacted with H_2S but yielded no identifiable products: these two ions were stable in argon at 1×10^{-5} Pa, but in the presence of H_2S their intensities diminished to zero in 0.4 s.

(*b*) The odd n ions from C_{15}^- to C_{25}^- inclusive showed no evidence of reaction with H_2S, and could be stored in the presence of H_2S for up to 50 s.

Table 1 Distribution of product types from reactions of carbon anions with H_2S as a function of n. **M** and **m** represent major and minor products, respectively

Eqn	Product	n 4	5	6	7	8	9	11	13
(3)	HS^-	**M**	**M**	**M**	**M**	**M**	**M**	**M**	**M**
(4)	C_nH^-	**M**	**m**	**M**	**M**	**M**	**M**	**m**	**m**
(5)	C_nHS^-	**m**	**M**	**m**	**m**	**m**	**m**		
(6)	$C_nH_2S^-$						**m**	**M**	**m**
(7)[a]	$C_nH_3S^-$					**M**			
(8)[a]	$C_nH_3S_2^-$						**m**		
(9)[a]	$C_{n-1}H_3S^-$						**M**	**m**	**m**
(10)[a]	$C_{n-4}S_2^-$				**M**		**M**		
(11)	$C_{n-1}H^-$				**m**		**M**		

[a] Product from a secondary reaction.

(*c*) For all of the C_n^- anions that reacted with H_2S (except C_{10}^- and C_{12}^-), deprotonation was a significant pathway because HS^- was of major intensity ($>10\%$).

(*d*) Abstraction of an H atom from H_2S to generate C_nH^- occurred as a major pathway ($>10\%$) for $n = 4, 6, 8$, but the ions C_nH^- appeared with only minor intensity ($<10\%$) for n odd [eqn. (4)].

(*e*) The addition of H and S to C_n^- to form C_nHS^- was a major pathway for $n = 5$, but a minor one for $n = 4, 6, 7, 8$ and 9.

(*f*) Complete addition of H_2S to form $C_nH_2S^-$was observed to give major ion intensity only for $n = 11$, and minor intensity for $n = 9, 13$.

(*g*) The formation of $C_nH_3S^-$ was observed only for $n = 8$. However, $C_{n-1}H_3S^-$ ions were generated in the reaction of C_n^- with H_2S for $n = 9$, 11 and 13 [eqn (9)].

(*h*) C–C bonds were broken in the formation of $C_3S_2^-$ as a major product from C_7^- and a minor product from C_9^-. A major product of the reaction of C_9^- with H_2S was $C_5S_2^-$. These are the two examples of reaction type (10).

(*i*) The formation of C_8H^- from C_9^- and of C_6H^- from C_7^- [eqn (11)] must involve the formation of HCS, the thioformyl radical recently proposed to be involved in the collision of the comet Shoemaker–Levy with Jupiter.[15]

$$C_9^- + H_2S \rightarrow C_8H^- + HCS$$

(*j*) Only one ion of type $C_nH_3S_2^-$ was observed, as a minor product with $n = 9$ [eqn (8)].

Some information about the temporal course of these multiple reactions has been obtained. The time courses of the reactions of C_8^- and C_9^- with H_2S have previously been reported.[9] The reactions of C_n^- with H_2S obeyed pseudo first-order kinetics for $n = 4$–9, but not for $n = 11$ or 13. The C_{11}^- and C_{13}^- anions initially reacted quite rapidly with H_2S but even for reaction times longer than 10 s some of the carbon anions remained unreacted. Fig. 1 shows the evolution of products in the reaction of C_{13}^- with H_2S. It is significant that only about 50% of the C_{13}^- reacts, forming $C_{13}H^-$ and HS^- in the early stages, followed by $C_{13}H_2S^-$ and $C_{12}H_3S^-$ from a secondary reaction of $C_{13}H^-$.

Reactions with benzenethiol

Products of the reactions of C_n^- with PhSH are listed in Table 2. The major product ion in all cases, except for $n = 11$, 13 and 15, was the phenylthiolate anion PhS^-. Fig. 2 shows the product ions for the reaction of C_{11}^- with benzenethiol after a reaction time of 3 s. The reactions of the large C_n^- anions (n odd > 15) were very slow and even after 20 s the product PhS^- had only minor intensity for C_{17} to C_{25}. The C_{19} anion shows some enhanced reactivity by the formation of the addition product, $C_{19}PhSH^-$.

The types of product ions containing carbon are C_nH^-($n = 4, 11, 13$), $C_nH_2^-$ ($n = 13$), C_nSH^- ($n = 4$–8), C_nPhSH^- ($n = 7, 9, 11, 19$), $C_nPhSH_2^-$ ($n = 9, 11, 13, 15$). It is evident that PhSH is functioning as an H atom transfer reagent, SH transfer reagent, and is also adding to C_n^-. This is comparable with

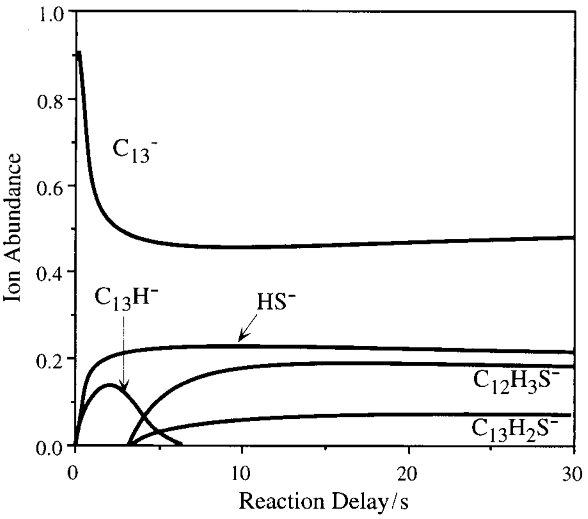

Fig. 1 Time course of the distribution of ions during reaction of C_{13}^- and H_2S.

Table 2 Product ions of the reactions of carbon anions with benzenethiol: $C_n^- + PhSH$

n	Major product	Minor products
4	PhS^-	C_4H^-, C_4SH^-
5	PhS^-	C_5SH^-
6	PhS^-	
7	PhS^-	C_7PhSH^-
8	PhS^-	C_8SH^-
9	PhS^-	C_9PhSH^-, $C_9PhSH_2^-$
10	PhS^-	
11	$C_{11}PhSH_2^-$[a]	$C_{11}PhSH^-$, PhS^-, $C_{11}H^-$
12	PhS^-	
13	$C_{13}PhSH_2^-$[a]	$C_{13}H^-$, $C_{13}H_2^-$,[a] PhS^-
15	$C_{15}PhSH_2^-$	PhS^-
17	PhS^-	
19	PhS^-	$C_{19}PhSH^-$
21	PhS^-	
23	PhS^-	
25	PhS^-	

[a] Secondary product.

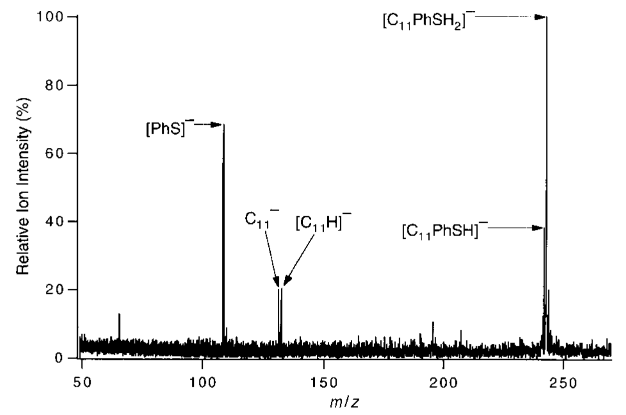

Fig. 2 Mass spectrum of the products of reaction of C_{11}^- with benzenethiol (PhSH) after 3 s reaction time.

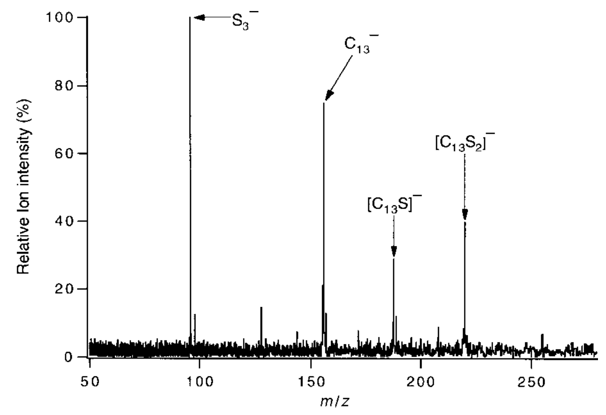

Fig. 3 Mass spectrum of the reaction mixture after 10 s in the reaction of C_{13}^- with S_8.

the reactions of H_2S described above, and there are some analogies: $C_nH_2S^- \equiv C_nPhSH^-$ and $C_nH_3S^- \equiv C_nPhSH_2^-$.

Reactions with sulfur, S_8

The products of the reactions of C_n^- anions with S_8 are listed in Table 3. Sulfur is more reactive than H_2S or P_4[10] as shown by its reactivity with all the ions: formation of S_3^- occurred for all the carbon anions studied. The observation of the reaction of C_8^- was hampered by the mass of C_8^- having the same mass as S_3^-, and the product ions C_8S^- and $C_8S_2^-$ having the same masses as S_4^- and S_5^-, respectively. The carbon sulfide ions could be differentiated from the sulfide ions by the observation of the ^{13}C isotopomer signal.

The well-known S_3^- ion was a major product of the reactions of S_8 with C_n^- anions, $n = 5$, 7–13, and 15–25 (n odd), but S_3^- was a minor product in the reactions of C_4^- and C_6^-. Instead, the ions $C_4S_2^-$ and $C_6S_2^-$ were observed to be the major product in the latter reactions.

In general, reaction (12) occurred first, followed by reaction (13), leading to formation of the product $C_nS_2^-$.

$$C_n^- + S_8 \rightarrow C_nS^- \quad (12)$$

$$C_nS^- + S_8 \rightarrow C_nS_2^- \quad (13)$$

Fig. 3 shows the formation of S_3^-, $C_{13}S^-$ and $C_{13}S_2^-$ in the reaction of C_{13}^- with S_8. Additional products appeared in the reaction of C_4^- with S_8, as shown in Fig. 4, including $C_4S_3^-$, which was the only product with more than two S atoms observed in our study. C_4^- and C_{12}^- gave small amounts of C_nSH^-. No addition products were observed for the larger ions C_{17}^-, C_{21}^-, C_{23}^- and C_{25}^-, although $C_{19}S^-$ was observed as a minor product, indicating the enhanced reactivity of C_{19}^-. During the reactions of the carbon anions with S_8, products such as $[C_4SH]^-$ and $[C_{12}SH]^-$ were formed, possibly by reaction with background water in the cell.

Table 3 Product ions of the reactions of carbon anions with sulfur: $C_n^- + S_8$

n	Major products	Minor products	Trace products
4	$C_4S_2^-$	S_3^-, C_4S, C_4HS^-, $C_4S_3^-$, S_4^-	S_n^- ($n = 5$–8)
5	S_3^-	S_n^- ($n = 5$–8), C_5S^-, $C_5S_2^-$	
6	$C_6S_2^-$	S_3^-, C_6S^-	S_n^- ($n = 4$–8)
7	S_3^-	C_7S^-, $C_7S_2^-$	S_n^- ($n = 4$–8)
8	S_3^-	C_8S^-, $C_8S_2^-$	
9	S_3^-	C_9S^-, $C_9S_2^-$	S_n^- ($n = 4$–8)
10	S_3^-	$C_{10}S^-$, $C_{10}S_2^-$	S_n^- ($n = 4$–8)
11	S_3^-	$C_{11}S^-$, $C_{11}S_2^-$	S_n^- ($n = 4$–8)
12	S_3^-	$C_{12}S^-$, $C_{12}S_2$	S_n^- ($n = 4$–8)
13	S_3^-	$C_{13}S^-$, $C_{13}S_2^-$	S_4^-
15	S_3^-	$C_{15}S^-$, $C_{15}S_2^-$	
17	S_3^-		S_4^-
19	S_3^-	$C_{19}S^-$	
21	S_3^-		
23	S_3^-		
25	S_3^-		

The properties of $C_4S_2^-$ and $C_6S_2^-$ were probed by collision-induced dissociation (CID), which yielded C_n^- and C_nS^- ($n = 4$, 6). Low-energy CID gave C_nS^- as the major initial product ion and at higher collision energies C_n^- became more intense.

Discussion

General observations on the gas phase reactions

The laser ablation process produces highly energetic ions that cool as the laser plume expands. The ions are trapped and undergo collisions with the neutral molecules in the cell. Each collision reduces the translational energy of the ion and also decreases the collision rate and so it is difficult to estimate the translation energy of an ion selected after a given time. With a pressure of 1×10^{-5} Pa of reagent gas, each ion may undergo an estimated ~10–30 collisions per second. An ion of mass 48 (C_4) will lose more than 50% of the total translational energy per collision with argon (mass 40) and so will be approaching the translational energy of the molecules in the cell, that is room temperature.

A second problem arises: are all the ions in their ground state? Collisions with an atomic gas such as argon may not supply suitable pathways for excited ions to lose electronic energy to attain the ground state but with reactive molecules such as S_8 or H_2S there should be such pathways. Very reactive ions will have formed products before selection of the C_n^-

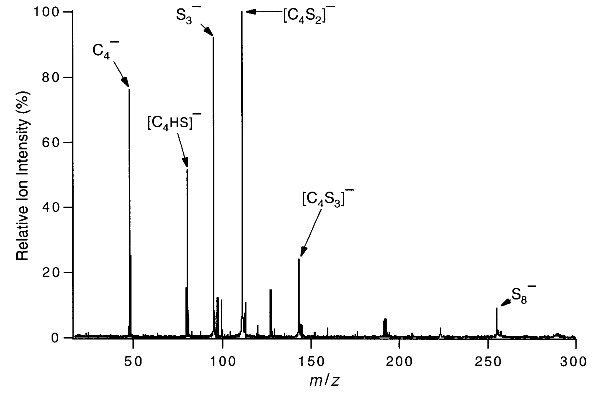

Fig. 4 Mass spectrum of the mixture of ions after reaction of C_4^- with S_8 for 5 s.

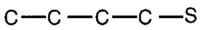

1

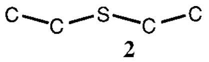

2

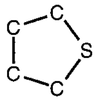

3

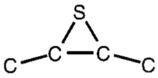

4

5

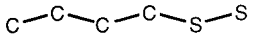

6

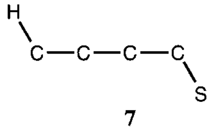

7

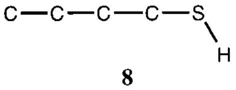

8

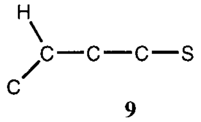

9

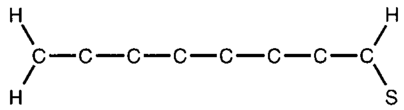

10

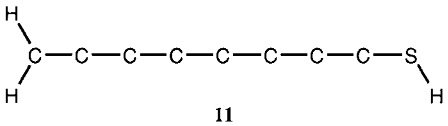

11

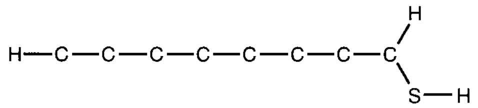

12

anion. Thus, we believe the ions selected are in their ground state and have energies close to molecules at room temperature.

The C_n^- anions, although regarded as less reactive than the similar carbon cations, do react with sulfur-containing molecules whereas no reactivity has been observed with H_2O[6] and only limited reactivity with O_2.[8] The rates of reaction of the C_n^- anions with sulfur molecules generally decrease as n increases, as was observed previously for reactions with P_4.[10] The sequential addition of sulfur atoms to the carbon chains is borne out by the collision-induced dissociation experiments, which indicate that the two sulfur atoms in $C_4S_2^-$ and $C_6S_2^-$ are removed as single S atoms rather than as an S_2 unit. A general observation is that the C_n^- anions are more reactive with S_8 and PhSH than with H_2S. The larger C_n^- anions ($n > 13$) show no reactivity towards H_2S but do show reactivity towards S_8 and PhSH.

These results pose some questions such as:

(*a*) Why do the sulfur compounds have increased reactivity compared with homologous oxygen reactants?

(*b*) What are the probable geometric and electronic structures of the products?

(*c*) How can the reactivities be understood?

(*d*) What is happening with C_{10} and C_{12} and why are they different?

Lagow et al[17] have observed that carbon allotropes $-(C{\equiv}C)_n-$ are stabilized by capping end groups and so the reactions of small linear carbon anions with hetero atoms would likely occur by addition at each end of the carbon chain.

McElvaney[6] reported that the small carbon anions were unreactive to oxygen. Although Watanabe *et al.*[8] observed some reaction of O_2 with some small carbon anions, they carried out the reactions at much higher pressures. The increased reactivity of S_8 is probably due to a combination of two factors, the lower bond energy of the S–S bond compared to the O–O bond (425 and 498 kJ mol^{-1}, respectively) and the larger cross section of the 'floppy' sulfur molecule.

Bond energies and cross section are also probably the two major factors in the enhanced reactivity of H_2S compared with H_2O. The bond dissociation energies of HS–H and HO–H are 382 and 498 kJ mol^{-1}, respectively. The bond dissociation energy of PhS–H, 349 kJ mol^{-1}, is lower than the S–S bond energy of S_8 and the S–H bond energy of H_2S and so PhSH might be expected to be more reactive with C_n^- than the other two reagents.

In an attempt to answer questions (*b*) to (*d*) we have resorted to density functional theory to calculate some of the properties of the reaction products.

Density functional calculations

Non-local density functional methods[18] were used to explore the geometries, electronic structures, charge distributions, and electron affinities of some of the observed ions. For the species $C_nS^{-,0}$ ($4 \leqslant n \leqslant 9$) the geometries investigated included extended chains with the S atom terminal (such as **1**) or central (such as **2**), planar and non-planar cycles such as **3**, and thioepoxide structures such as **4**. For $C_nS_2^{-,0}$ the structural postulates involved S atoms at each end of an extended chain (such as **5**) or as S_2 at one end of the chain (such as **6**). Linear chains were not assumed, and the geometry optimizations did not impose symmetry constraints.

For both $C_nS^{-,0}$ and $C_nS_2^{-,0}$ the lowest energy-optimized structures were linear, with terminal S atoms and a slight increase of energy per atom as the C_n chain increased in length, as shown in Table 4. Alternative structures such as **2**, **3** and **4** were hundreds of kJ mol^{-1} less stable than **1**, and structures such as **6** were hundreds of kJ mol^{-1} less stable than **5**. As an example of the stability of the extended chains, Fig. 5 illustrates the course of the energy minimization of the cyclic postulate for $C_5S_2^-$.

Worth special mention is the $C_4S_3^-$ anion, which is linear and shows a long S–S bond and C–S bonds slightly longer than those observed in the C_nS^- and $C_nS_2^-$ anions. The carbon chain is similar to C_4S^- and SC_4S^- in that the central carbon–carbon bond is long. The neutral molecule C_4S_3 has shorter S–S and C–S bond lengths and the C–C bond lengths show smaller differences.

The lowest energy structures of the species $HC_nS^{-,0}$ ($4 \leqslant n \leqslant 9$) were also linear, with the H and S atoms connected at opposite ends of the C_n chain as shown in Table 5. Other structures that were investigated included the bent isomer **7**, the C_nSH connectivity **8** (*ca.* 180 kJ mol^{-1} less stable), and isomers with the H connected at non-terminal atoms, such as **9** (> 170 kJ mol^{-1} less stable).

In our experiments we have observed HC_nS^- from C_n^- where n is both even and odd but Zheng and coworkers[19] only observed similar anions for n even (for n odd these were of very low intensity). The linear H–C_n–S structures are in agreement with Zheng and colleagues but our carbon–carbon bond lengths are not in general agreement. Our calculated energy per atom in the anions also shows a steady increase as the value of n increases whereas those of Zheng and coworkers have an opposite trend. Both sets of calculations show similar trends in the electron affinities (where higher values are obtained for n being even) but our values are considerably higher than those of Zheng and coworkers.

Having established the most stable connectivities and linear geometries for C_nS, SC_nS, and HC_nS, as both anions and neutral molecules, we enquire about their electronic structures. A key property is the alternation of the electron affinities (Tables 4 and 5), being >0.5 eV larger for n even than for the adjacent n odd. This behaviour is plotted in Fig. 6, in com-

Table 4 Lowest energy structures for the anions and neutral molecules C_nS, C_nS_2 ($n = 4$–9) and C_4S_3

		Anion		Neutral		
Composition	Geometry[a]	Total energy/ kJ mol^{-1} (energy per atom)	Bond lengths/ Å[b]	Total energy/ kJ mol^{-1} (energy per atom)	Bond lengths/ Å[b]	Adiabatic EA/ kJ mol^{-1} (eV)
C_4S	C_4–S	−2764.0 (552.8)	S–C 1.64; C–C 1.27, 1.34, 1.30	−2486.6 (497.3)	S–C 1.58; C–C 1.30, 1.30, 1.33	277.4 (2.88)
C_5S	C_5–S	−3408.3 (568.0)	S–C 1.62; C–C 1.29, 1.30, 1.32, 1.30	−3210 (535.0)	S–C 1.57; C–C 1.30, 1.28, 1.31, 1.30	198.3 (2.06)
C_6S	C_6–S	−4081.1 (589.8)	S–C 1.63; C–C 1.28, 1.32, 1.27, 1.34, 1.30	−3774.8 (359.3)	S–C 1.58; C–C 1.29, 1.29, 1.29, 1.30, 1.32	306.3 (3.18)
C_7S	C_7–S	−4718.3 (589.8)	S–C 1.62; C–C 1.28, 1.30, 1.30, 1.29, 1.32, 1.30	−4479.8 (560.0)	S–C 1.58; C–C 1.29, 1.29, 1.30, 1.28, 1.31, 1.30	238.5 (2.47)
C_8S	C_8–S	−5386.1 (598.5)	S–C 1.62; C–C 1.28, 1.32, 1.28, 1.32, 1.28, 1.33, 1.30	−5055.9 (561.8)	S–C 1.58; C–C 1.29, 1.29, 1.29, 1.29, 1.29, 1.30, 1.32	330.2 (3.47)
C_9S	C_9–S	−6020.8 (602.1)	S–C 1.61; C–C 1.28, 1.30, 1.29, 1.29, 1.30, 1.28, 1.32, 1.30	−5748.8 (574.9)	S–C 1.58; C–C 1.29, 1.29, 1.29, 1.28, 1.30, 1.28, 1.31, 1.30	272.0 (2.82)
C_4S_2	S–C_4–S	−3229.6 (538.3)	S–C 1.64; C–C 1.27, 1.33, 1.27	−2994.9 (499.2)	S–C 1.59; C–C all 1.29	234.7 (2.43)
C_5S_2	S–C_5–S	−3874.0 (553.4)	S–C 1.63; C–C 1.28, 1.30, 1.28, 1.30	−3707.0 (529.6)	S–C 1.58; C–C all 1.29	167.0 (1.73)
C_6S_2	S–C_6–S	−4540.9 (567.6)	S–C 1.63; C–C 1.27, 1.32, 1.27, 1.32, 1.27	−4277.3 (534.7)	S–C 1.58; C–C all 1.29	263.6 (2.73)
C_7S_2	S–C_7–S	−5183.1 (575.9)	S–C 1.62; C–C 1.28, 1.31, 1.29, 1.29, 1.31, 1.28	−4976.9 (553.0)	S–C 1.59; C–C all 1.29	206.2 (2.14)
C_8S_2	S–C_8–S	−5845.0 (584.5)	S–C 1.62; C–C 1.28, 1.32, 1.28, 1.32, 1.28, 1.32, 1.28	−5562.6 (556.3)	S–C 1.59; C–C all 1.29	282.4 (2.93)
C_9S_2	S–C_9–S	−6492.3 (590.2)	S–C 1.61; C–C 1.28, 1.31, 1.29, 1.30, 1.30, 1.29, 1.31, 1.28	−6248.4 (568.0)	S–C 1.58; C–C all 1.29	243.9 (2.53)
C_4S_3	S–C_4–S–S	−3471.9 (496.0)	S–C 1.66, 1.63; C–C 1.27, 1.33, 1.27; S–S 2.07	−3192.0 (456.0)	S–C 1.63, 1.59; C–C 1.28, 1.30, 1.29; S–S 2.01	279.9 (2.90)

[a] All the optimized structures for both neutral and anionic species are linear. [b] The C–C bond lengths for C_nS are shown such that S is attached to C_1 and the first C–C bond length is C_1–C_2. Both C–S bond lengths are the same in SC_nS and only shown once; all the C–C bond lengths are given in a manner similar to C_nS. The C_4S_3 species bond lengths are arranged such that the first C–S bond length is S–C_1 and the S_2 group is at the other end of the molecule.

Table 5 The energies, bond lengths and electron affinities of the anionic and neutral linear HC_nS species ($n = 4$–9)

	Anion		Neutral		
Composition	Total energy/ kJ mol^{-1} (energy per atom)	Bond lengths/ Å[a]	Total energy/ kJ mol^{-1} (energy per atom)	Bond lengths/ Å[a]	Adiabatic EA/ kJ mol^{-1} (eV)
HC_4S	−3174.4 (529.1)	H–C 1.08; C–C 1.25, 1.35, 1.26; C–S 1.65	−2918.3 (486.4)	H–C 1.09; C–C 1.24, 1.34, 1.27; C–S 1.61	256.1 (2.65)
HC_5S	−3724.2 (532.0)	H–C 1.09; C–C 1.27, 1.32, 1.30, 1.29; C–S 1.63	−3548.9 (507.0)	H–C 1.09; C–C 1.24, 1.33, 1.27, 1.30; C–S 1.58	175.3 (1.82)
HC_6S	−4486.5 (560.8)	H–C 1.08; C–C 1.25, 1.35, 1.26, 1.34, 1.27; C–S 1.64	−4206.2 (525.8)	H–C 1.09; C–C 1.24, 1.34, 1.26, 1.31, 1.28; C–S 1.60	280.3 (2.91)
HC_7S	−5054.7 (561.9)	H–C 109; C–C 1.26, 1.33, 1.29, 1.30, 1.31, 1.28; C–S 1.62	−4839.6 (537.7)	H–C 1.09; C–C 1.24, 1.34, 1.27, 1.31, 1.28, 1.30; C–S 1.59	215.1 (2.23)
HC_8S	−5790.7 (579.1)	H–C 1.087; C–C 1.24, 1.35, 1.26, 1.33, 1.27, 1.33, 1.27; C–S 1.63	−5490.2 (549.0)	H–C 1.09; C–C 1.24, 1.34, 1.26, 1.32, 1.27, 1.31, 1.28; C–S 1.59	300.5 (3.11)
HC_9S	−6370.1 (579.1)	H–C 1.09; C–C 1.25, 1.34, 1.28, 1.31, 1.29, 1.29 1.31, 1.28; C–S 1.62	−6125.4 (556.9)	H–C 1.09; C–C 1.24, 1.34, 1.26, 1.32, 1.27, 1.30, 1.28, 1.29; C–S 1.58	244.7 (2.54)

[a] Bond lengths for HC_nS species are H–C_1 and then the carbon bonds start with C_1–C_2 until the final bond is the C_n–S bond.

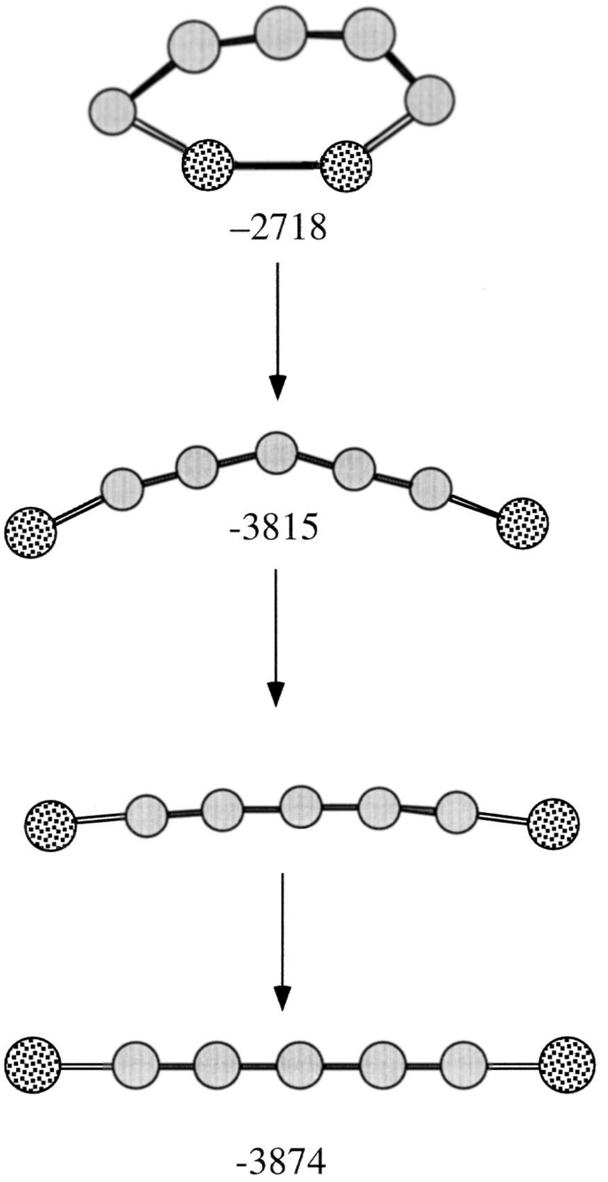

Fig. 5 Stages during the energy minimization calculation for $C_5S_2^-$. The energies of the structures are shown in kJ mol^{-1}.

parison with the electron affinities of the parent C_n chains. The electron affinities for the three types of heteroatom-terminated carbon chains follow the same general alternation as the C_n chains, but are appreciably smaller. The electron affinities for any value of n decrease in the sequence $C_n \gg$ $C_nS > HC_nS > SC_nS$, consistent with increased electron delocalization. There is a significant trend of increasing electron affinity with increasing n.

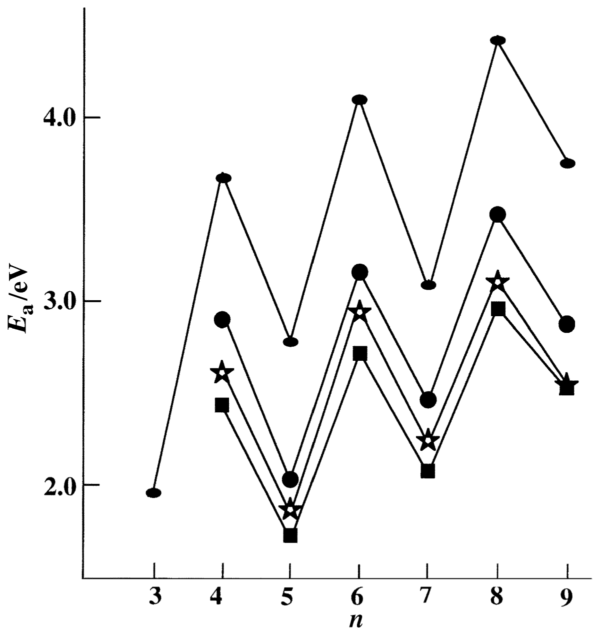

Fig. 6 The electron affinities (in eV) for (⬬) C_n (exptal[1]), (●) C_nS, (■) SC_nS and (★) HC_nS (calcd).

The calculated atom partial charges, using the Mulliken method, place the largest negative charge on terminal atoms of the chains: examples are $S^{-0.40}$ and terminal-$C^{-0.36}$ in C_4S^-, $S^{-0.32}$ and terminal-$C^{-0.29}$ in C_9S^-, $S^{-0.40}$ in SC_4S^-, and $S^{-0.35}$ in SC_9S^-.

An indicator of the electronic structure of these linear chain molecules is the differentiation of successive C–C bond distances, according to the extreme concepts of polycumulenic … C=C=C=C=C … or polyacetylenic … C≡C–C≡C–C … bonding. As is evident from Table 4, alternating C–C distances in any of the $C_nS^{-,0}$ or $SC_nS^{-,0}$ species generally vary by <0.04 to Å, with a maximum differentiation of 0.07 Å in C_6S^- and smaller variations in the neutral molecules. The electronic structures of these molecules are approximately polycumulenic. There is greater differentiation of C–C distances in $HC_nS^{-,0}$ (Table 5), particularly at the hydrogen end of the chain where the electronic structure is closer to H–C≡C–. For the HC_nS^- species where n is even the electronic structure approaches $H{-}C{\equiv}(C{-}C{\equiv})_xC{-}S$.

For the more hydrogenated species $C_nH_3S^-$ there is a wider range of possible connectivities. We investigated three of the possibilities for $C_8H_3S^-$, namely **10**, **11**, and **12**, with the

Table 6 Calculated energies (in kJ mol^{-1}) of the reactions of C_n^- with H_2S forming HS^-: $C_n^- + H_2S \rightarrow C_nH + HS^-$

n	$E(C_n^- + H_2S)$	$E(C_nH + HS^-)$	ΔE	C_n structure
4	−3034.6	−3145.1	−110.5	Linear
5	−3678.6	−3738.4	−59.8	Linear
6	−4354.3	−4450.1	−95.8	Linear
7	−4992.8	−5035.9	−43.1	Linear
8	−5658.4	−5736.7	−78.3	Linear
	−5240.5	−5440.0	−199.5	Cyclic
9	−6291.1	−6339.6	−48.5	Linear
	−6145.9	−6204.5	−58.6	Cyclic
10	−6957.6	−7031.6	−74.0	Linear
	−6897.3	−6984.4	−87.1	Cyclic
11	−7595.2	−7625.3	−30.1	Linear
	−7501.5	−7555.0	−53.6	Cyclic
12	−8239.6	−8305.7	−66.1	Linear
	−8157.5	−8167.2	−9.7	Cyclic
13	−8885.1	−8909.0	−23.9	Linear
	−8901.0	−8915.3	−14.3	Cyclic

Table 7 Comparison of the calculated bond lengths in C_nO with those of other calculations and values obtained from rotational spectra

n	C–O	C_1–C_2	C_2–C_3	C_3–C_4	C_4–C_5	C_5–C_6	C_6–C_7	C_7–C_8	C_8–C_9
4	1.19 (1.18^a)	1.31 (1.29^a)	1.29 (1.29^a)	1.34 (1.31^a)					
5	1.19 (1.17^a) (1.16^b) (1.16^c)	1.30 (1.29^a) (1.26^b) (1.28^c)	1.28 (1.27^a) (1.29^b) (1.26^c)	1.31 (1.30^a) (1.29^b) (1.29^c)	1.30 (1.29^a) (1.27^b) (1.28^c)				
6	1.19 (1.18^a)	1.30 (1.29^a)	1.29 (1.29^a)	1.30 (1.28^a)	1.30 (1.30^a)	1.33 (1.31^a)			
7	1.19 (1.18^a)	1.30 (1.29^a)	1.28 (1.28^a)	1.30 (1.29^a)	1.28 (1.27^a)	1.31 (1.30^a)	1.30 (1.29^a)		
8	1.19 (1.18^a)	1.30 (1.29^a)	1.29 (1.28^a)	1.30 (1.28^a)	1.29 (1.29^a)	1.29 (1.28^a)	1.30 (1.30^a)	1.32 (1.31^a)	
9	1.19 (1.18^a)	1.30 (1.29^a)	1.29 (1.28^a)	1.29 (1.29^a)	1.29 (1.28^a)	1.30 (1.29^a)	1.28 (1.28^a)	1.31 (1.30^a)	1.30 (1.29^a)

[a] Ref. 19. [b] Ref. 20. [c] Ref. 21.

result that **10** is most stable with **11** less stable by *ca.* 100 kJ mol^{-1}, and **12** is 120 kJ mol^{-1} less stable than **10**.

Energies involved in reactions of the carbon anions with H_2S

With respect to the reactions of the carbon anions with H_2S, HS^- was a major product for the anions C_n^- where $n = 4$–9, 11 and 13:

$$C_n^- + HSH \rightarrow C_nH + HS^- \qquad (14)$$

The energies of reaction (ΔE) of C_n^- with H_2S are all exothermic as shown in Table 6. In this table the optimized structures of the reactants C_n^- and H_2S were taken and placed 10 Å apart; the total energy of the reactants, $E(C_n^- + H_2S)$, was then calculated. The total energy of the products, $E(C_nH + HS^-)$, was calculated by a similar process. The energy of the reaction was taken as the difference between the total energy of the products and the total energy of the reactants: $\Delta E = E(C_nH + HS^-) - E(C_n^- + H_2S)$. The values for C_{10}^- and C_{12}^- have been calculated even though no products were observed in the reaction of these ions with H_2S. The reaction energies show that for the linear C_n^- isomers there is an even-odd variation with the higher values for the n even ions. The reaction energies also show a general decrease with increasing values of n, paralleling the decrease in the rates of reaction.[9]

The reaction energies of the cyclic isomers, which might be expected to be more important for $n > 9$, are larger than those of the linear isomers for $n = 8$–11, but smaller for $n = 12$ and 13. The reaction energy of the cyclic C_8^- is surprisingly large. The energies of the cyclic C_8^- and C_8H (−4604.6 and −4772.3 kJ mol^{-1}, respectively) indicate that the cyclic isomers are less stable than the corresponding linear isomers (−4913.3 and −4983.1 kJ mol^{-1} for C_8^- and C_8H, respectively) but the energy difference between the cyclic C_8^- and C_8H is much larger than the difference in the linear isomers. Our calculations indicate that the linear isomers of C_n^- are more stable than the cyclic isomers except for C_{13}^- and the cyclic isomers of $C_{10}H$, $C_{11}H$ and $C_{13}H$ are more stable than their linear counterparts.

Generally, the total energies of both the reactants and products for most of the cyclic isomers are lower than the values for the linear isomers except where $n = 13$.

The reactions of C_{10}^- and C_{12}^- with H_2S

Both C_{10}^- and C_{12}^- react with H_2S but there are no observable product ions. There are two possible explanations:

(*a*) The process could involve production of the hydride ion (which could not be detected in the FTICR) by the reaction

$$C_n^- + H_2S \rightarrow C_nSH + H^-$$

The hydride ion might be expected to react with H_2S to form H_3S^-, which would probably eliminate H_2 to give HS^-. Our calculations indicate that H_3S^- is less stable than H_2S.

(*b*) The process could involve electron loss caused by ion-molecule collisions. The electrons could be trapped in the cell and would be unobservable (under our experimental conditions). The formation of H_2S^- seems unlikely as this ion is calculated to have a negative electron affinity. The vertical electron affinities of 2.30 and 2.55 eV for C_{10} and C_{12}, respectively, measured by Smalley and coworkers,[1] are the lowest in the series C_2–C_{13}, with the exception of C_3. The electron affinities of the odd-numbered carbon systems from C_{15} to C_{25} are also larger than those for C_{10} and C_{12}.

Process (*b*) would seem the most likely explanation for the non-observance of product ions. C_{10}^- and C_{12}^- do react with PhSH to produce the PhS^- anion and this could be due to the lower H–S bond energy in benzenethiol.

It is of interest that although C_{10}^- and C_{12}^- do not react with H_2S, the ions $C_{10}H_3S^-$ and $C_{12}H_3S^-$ are observed as minor products in the reactions of C_{11}^- and C_{13}^- with H_2S.

Summary

Our general conclusions are that the carbon anions are more reactive with S_8 and PhSH than with H_2S or P_4. The reactions of H_2S with the C_{odd}^- anions generally produce more product ions than reaction with C_{even}^- anions. The reactions of S_8 with the C_n^- anions generally produce S_3^-, except for C_4^- and C_6^- where the $C_nS_2^-$ anions are the major product ions. The addition of sulfur atoms appears to be sequential and the resultant $C_nS_2^-$ anions have no S–S interaction. PhSH is reactive with all the carbon anions studied and C_{11}^-, C_{13}^- and C_{15}^- produce addition products as major ions.

DFT calculations indicate that the C_nS^- anions are linear and delocalized, approaching a cumulene-type structure. The SC_nS^- anions also have similar linear delocalized structures. The linear HC_nS^- anions have structures in which the carbon bonded to the hydrogen is more acetylenic while subsequent C–C bonds and the C–S bond are closer to double bonds. Predominant canonical representations of C_4 species are shown below:

C=C=C=C=S S=C=C=C=C=S H–C≡C–C=C=S

The unprecedented species C_4S_3 is a linear SC_4S–S molecule with a single bond between the two end sulfur atoms. Thus linear geometries are a general feature for heteroatom-substituted carbon chains C_nX and C_nX_2 where X = O, S, N, P, Si, and $n = 4$–9.

Finally, one of the important product ions formed in the reactions of C_8^- and C_9^-, $C_8H_3S^-$, has a planar structure with a linear carbon chain and a CH_2 group at one end of the ion, the carbon at the other end is bonded to a hydrogen and a sulfur atom. It is probable that the ions $C_{10}H_3S^-$ and $C_{12}H_3S^-$ have similar structures.

Experimental

The reactions of carbon anions with sulfur molecules were studied by Fourier transform mass spectrometry using methods previously described.[9,20]

The carbon anions were produced by laser ablation of graphite or petroleum coke using pulses from a Nd-YAG laser at the fundamental frequency, 1064 nm. After ablation the ions were stored for a minimum of 1 s (cooling time) before selection of the required C_n^- anion. The carbon anions C_n^- (even $n = 14$–24) were of low abundance, compared with the odd-numbered species of similar size, and could not be isolated for reaction. The H_2S or benzenethiol was admitted to the cell *via* a molecular leak valve to maintain an uncorrected pressure of 1×10^{-5} Pa. The H_2S and benzenethiol (PhSH) used in this study were commercial samples checked for purity by electron impact mass spectrometry. Sulfur vapor was introduced into the cell by sublimation from a capillary tube containing $S_{8(s)}$ attached to the probe tip.[20] The sublimation of the S_8 maintained a pressure of $1\text{–}2 \times 10^{-6}$ Pa, to which was added argon to maintain an overall pressure of 1×10^{-5} Pa.

Collision-induced dissociation (CID) studies of $C_4S_2^-$ and $C_6S_2^-$ were performed in the presence of argon and S_8 with a total pressure of 2×10^{-5} Pa, under conditions similar to those for the carbon phosphide anions.[10]

Density functional calculations were spin unrestricted using the BLYP functional with double numerical basis sets, non-local corrections and frozen core orbitals, as implemented in the program DMOL.[18] Our density functional calculations were evaluated by comparison with experimental observations and *ab initio* calculations for comparable C_nO molecules. Table 7 compares the bond distances for C_nO ($4 \leqslant n \leqslant 9$) obtained by our DFT calculations. In general our C–O and C–C bond lengths agree with the other data[21,22,23] (both experimental and theoretical).

Acknowledgements

This research is funded by the Australian Research Council. F. Hopwood gratefully acknowledges an Australian Postgraduate Award (Industry) with COMALCO.

Notes and references

1 S. Yang, K. J. Taylor, M. J. Craycraft, J. Conceicao, C. L. Pettiette, O. Chesnovsky and R. E. Smalley, *Chem. Phys. Lett.*, 1988, **144**, 431; D. W. Arnold, S. E. Bradforth, T. N. Kitsopoulos and D. M. Neumark, *J. Chem. Phys.*, 1991, **95**, 8753; H. Handschuh, G. Gentefor, B. Kessler, P. S. Bechthold and W. Eberhardt, *Phys. Rev. Lett.*, 1995, **77**, 1095.

2 T. N. Kitsopoulos, C. J. Chick, Y. Zhao and D. M. Neumark, *J. Chem. Phys.*, 1991, **95**, 5479; D. W. Arnold, Y. Zhao, T. N. Kitsopoulos and D. M. Neumark, *J. Chem. Phys.*, 1992, **97**, 6121.

3 D. Forney, J. Fulara, P. Freivogel, M. Jakobi, D. Lessen and P. J. Maier, *J. Chem. Phys.*, 1995, **103**, 43; P. Freivogel, J. Fulara, M. Jakobi, D. Forney, and P. J. Maier, *J. Chem. Phys.*, 1995, **103**, 54; Y. Zhao, E. de Beer, C. Xu, T. Taylor and D. M. Neumark, *J. Chem. Phys.*, 1996, **105**, 4905.

4 G. von Helden, P. R. Kemper, N. G. Gotts and M. T. Bowers, *Science*, 1993, **259**, 1300; G. von Helden, M. T. Hsu, N. G. Gotts, P. R. Kemper and M. T. Bowers, *Chem.. Phys. Lett.*, 1993, **204**, 15.

5 J. D. Watts and R. J. Bartlett, *J. Chem. Phys.*, 1992, **97**, 3445; G. von Helden, W. E. Palke and M. T. Bowers, *Chem. Phys. Lett.*, 1993, **212**, 247; K. Raghavachari, *Z. Phys. D*, 1989, **12**, 61.

6 S. W. McElvany, *Int. J. Mass Spectrom. Ion. Process.*, 1990, **102**, 81.

7 J. Hutter, H. P. Luthi and F. Diedrich, *J. Am. Chem. Soc.*, 1994, **116**, 750.

8 N. Watanabe, H. Shiromaru, Y. Achiba, N. Kobayashi and Y. Kaneko, *Z. Phys. D*, 1991, **26**, 254.

9 F. G. Hopwood, K. J. Fisher, G. D. Willett and P. Greenhill, *Rapid Commun. Mass Spectrom.*, 1996, **10**, 110.

10 K. J. Fisher, I. G. Dance and G. D. Willett., *Eur. Mass Spectrom.*, 1996, **2**, 369; K. J. Fisher, I. G. Dance and G. D. Willett., *Eur. Mass Spectrom.*, 1997, **3**, 331.

11 R-B. Huang, C-R. Wang, Z-Y. Liu, L-S. Zheng, F. Qi, L-S. Sheng, S-Q. Yu and Y-W. Zhang, *Z. Phys. D* , 1995, **33**, 49; Z-C. Tang, R-B. Huang, L. Shi and L-S. Zheng, *Int. J. Mass Spectrom. Ion. Process.*, 1998, **173**, 71.

12 S. Hunsicker and R. O. Jones, *J. Chem. Phys.*, 1996, **105**, 5048.

13 S. Lee, *Chem. Phys. Lett.*, 1997, **268**, 69.

14 D. A. Williams, *Chem. Eur. J.*, 1997, **3**, 1929; M. B. Bell, L. W. Avery and P. A. Feldman, *Astrophys. J.*, 1993, **417**, L37.

15 R. I. Kaiser, C. Ochsenfeld, M. Head-Gordon and Y. T. Lee, *Science*, 1998, **279**, 1181.

16 J. G. Breitzer, J. H. Chou and T. B. Rauchfuss, *Inorg. Chem.*, 1998, **37**, 2080.

17 R. L. Lagow, J. J. Kampa, H-C. Wei, S. L. Battle, J. W. Genge, D. A. Laude, C. J. Harper, R. Bau, R. C. Stevens, J. F. Haw and E. Munson, *Science*, 1995, **267**, 362.

18 DMOL, Biosym Technologies, Inc. San Diego CA, v2.3 and 2.36; B. Delley, M. Wrinn and H. P. Lüthi, *J. Chem. Phys.* , 1994, **100**, 5785. C. Lee, W. Yang and R. G. Parr, *Phys. Rev. B* , 1988, **37**, 785; A. D. Becke, *Phys. Rev. A* , 1988, **38**, 3098.

19 Z-Y. Liu, Z-C. Tang, R-B. Huang, Q. Zhang and L-S. Zheng, *J. Phys. Chem. A*, 1997, **101**, 4019.

20 K. J. Fisher, I. G. Dance and G. D. Willett, *Inorg. Chem.*, 1996, **35**, 4177.

21 N. Moazzen-Ahmadi and F. Zerbetto, *J. Chem. Phys.*, 1995, **103**, 6343.

22 T. Ogata, Y. Oshima and Y. Endo, *J. Am. Chem. Soc.*, 1995, **117**, 3593.

23 P. Botschwina, J. Flügge and P. Sebald, *J. Phys. Chem.*, 1995, **99**, 9755.

Paper 9/00563C